JOURNAL OF ADVANCED TRANSPORTATION
J. Adv. Transp. 2012; **46**:161–176
Published online 9 November 2010 in Wiley Online Library (wileyonlinelibrary.com). DOI: 10.1002/atr.151

An intersection turning movement estimation procedure based on path flow estimator

Anthony Chen[1]*, Piya Chootinan[2], Seungkyu Ryu[1], Ming Lee[3] and Will Recker[4]

[1]*Department of Civil and Environmental Engineering, Utah State University Logan, UT 84322-4110, USA*
[2]*Bureau of Planning, Department of Highways, Bangkok 10400, Thailand*
[3]*Department of Civil and Environmental Engineering, University of Alaska, Fairbanks AK 99775-5900, USA*
[4]*Department of Civil Engineering, University of California, Irvine, CA 92697-3600, USA*

SUMMARY

Estimation of intersection turning movements is one of the key inputs required for a variety of transportation analysis, including intersection geometric design, signal timing design, traffic impact assessment, and transportation planning. Conventional approaches that use manual techniques for estimation of turning movements are insensitive to congestion. The drawbacks of the manual techniques can be amended by integrating a network traffic model with a computation procedure capable of estimating turning movements from a set of link traffic counts and intersection turning movement counts. This study proposes using the path flow estimator, originally used to estimate path flows (hence origin–destination flows), to derive not only complete link flows, but also turning movements for the whole road network given some counts at selected roads and intersections. Two case studies using actual traffic counts are used to demonstrate the proposed intersection turning movement estimation procedure. Copyright © 2010 John Wiley & Sons, Ltd.

KEY WORDS: transportation planning; network traffic model; turning movement estimation; path flow estimator

1. INTRODUCTION

Network traffic models (*i.e.*, the four-step modeling procedure) were originally developed to forecast link flows on the regional circulation network. In the past decade, with the ever-increasing availability of computer hardware and software, traffic models have been widely used by traffic engineers and regional planners. In addition, the increasing consciousness on environmental impacts has also prompted agencies to recommend the use of traffic models for the assessment of traffic impacts cumulated by continuous land use and network development on a 20–30 year horizon [1]. Traditionally, the estimation of future turning movements with a traffic model involves the application of factoring algorithms among which Furness Method [2] is the most commonly used. Regional traffic models first estimate future link volumes, in and out of an intersection, based on estimated future demands, which is in general difficult to obtain. Then, the base year turning movement counts at an intersection are multiplied by factors until the total inflows and outflows of the intersection closely match the estimated link volumes. An obvious limitation of the method is the inapplicability for intersections without existing turning counts. Although recent advanced traffic sensors (*e.g.*, video detection) have the potential to automate such data collection processes, it is still expensive to fully instrument every intersection with sensors. In addition, the Furness method assumes that future turning movements will be proportional to their existing turning counterparts. However, this is not the case when a major change occurs in the land use pattern and transportation system. In fact, the volume on a particular movement of an intersection that is on a new ''preferred'' path may dramatically increase due to the corresponding changes of travel behavior. Another approach to incorporating turning movement estimation with a traffic model is to estimate and calibrate a baseline trip table from existing traffic counts with a special computation procedure that can reproduce turning movements at key

*Correspondence to: Anthony Chen, Department of Civil and Environmental Engineering, Utah State University Logan, UT 84322-4110, USA. E-mail: anthony.chen@usu.edu

intersections. Implicit in the baseline trip table is the trip length distribution that reflects the destination and route choice behavior in the region. Future trip addition can be estimated and added to the baseline trip table. Turning movement forecasts can thus be obtained by assigning the future trip table to the future network. With such an approach, the forecasting of turning movements with a future trip table can account for the effects of both land use change and driver's path choice behavior sensitive to congestion and network changes.

Some earlier studies presented applicable procedures for turning movement estimation and calibration with network traffic counts. Jeffreys and Norman [3] discussed some general properties (*i.e.*, total inflow equals to total outflow, zero diagonal elements, etc.) required for the turning movement flow matrix to be realistic and feasible. They provided matrix manipulation schemes to generate additional feasible and realistic matrices from the initial feasible pattern. Later, most of studies on this topic have been focused on the application of mathematical models for identifying the most probable turning movement flow matrix of which the row and column sums, respectively, satisfy the known total inflow and outflow of intersection. Examples of these studies include Mekky [4], van Zuylen [5], Hauer *et al.* [6], Bell [7], Maher [8], Schaefer [9], and others.

Mekky [4] proposed a well-known log-linear model, which was derived as the solution to the constrained optimization problem (entropy maximization). Similar model was also obtained by van Zuylen [5] using the minimum information approach. Based on work of van Zuylen [5], the most probable matrix is defined by the matrix obtained with the minimum amount of information. Prior turning movement probabilities can also be incorporated in these models. As reported by van Zuylen [5] and some follow-up studies by Hauer *et al.* [6] and Schaefer [9], turning movement probabilities (relative size of turning movement volumes) heavily affect the accuracy of turning movement flow estimates and have been considered as one of critical inputs. This type of information is typically obtained based on either long-term or short-term historical traffic data. It has been reported that a higher degree of accuracy of turning movement flow estimate was obtained when turning movement probabilities were specified according to intersection type and approach type (*e.g.*, arterial or collector street) rather than the average value for each turning movement [6]. In addition, the solution based on historical data assumes that there is no substantial change in landuse or travel demand pattern. This assumption may not be applicable for long-range forecasting of turning movements [9].

Interestingly, two aforementioned models can be solved using similar balancing procedures, which resemble the Furness growth factor model [2]. The initial estimate of turning movement flows will iteratively be scaled up or down to produce the total observed inflow and outflow on all intersection's approaches. Several studies mentioned earlier have demonstrated the capability of these models in estimating the turning movement flow matrix of both a single intersection and a group of intersections in the network. However, in the later case, the estimation of turning movements for each intersection is performed independently as long as the observed inflow and outflow at each intersection is in equilibrium. There is no consideration put toward the relationship of traffic flow running through multiple intersections in the network.

Martin and Bell [10] adapted the network flow (NETFLO) algorithm, which is a linear programming originally developed for optimizing flows of water and electricity networks, to derive turning movements from traffic counts. As mentioned in their study, this technique cannot represent the behavior of road network's users as required in the conventional transportation modeling. However, with the ability of quick estimation, it might be useful for real-time transportation applications. Mathematically, the NETFLO algorithm is to minimize the summation of link flow estimates on all transportation links, which is not exactly the transportation cost. The general transportation network is expanded to properly represent all turning movements at each intersection. The flow continuities (flow conservations) at transportation nodes, including intersections, are modeled as a series of linear equations, while estimated link and turning movement flows must satisfy the set of constraints defined by measured link flows. In general, due to the variation of traffic measurements, it is difficult to fulfill flow continuity at every node. The requirement of flow continuity can be handled by the introduction of error arcs. The error arcs are used to retain a portion of inconsistent flows causing unsatisfied flow continuity. In a follow-up study by Martin [11], the NETFLO algorithm was further investigated for the capability in estimating turning movement flows within a shorter time period and the effects of several parameters associated with the model namely upper limits of flows on error arcs on the quality of estimation were also examined.

DOI: 10.1002/atr

Recently, Wu and Thnay [12] proposed the origin–destination (O–D) based method for estimating turning movements. Instead of estimating turning movements directly, they estimate the O–D matrix from a set of existing traffic and turning movement counts. Then, based on the current O–D matrix estimated, the future O–D matrix, obtained by the traditional travel demand model, is adjusted accordingly using the procedure similar to the Furness method. Finally, the adjusted future O–D matrix is assigned onto the network based on any user equilibrium principle to obtain both future link and turning movement flows. In their study, the gradient-based technique, which was developed by Spiess [13] and implemented in EMME/2 macro, was used as the O–D estimator. By coupling the travel demand model with O–D estimation, Wu and Thnay [12] reported that the proposed method could represent changes in travel demand (landuse) pattern more properly.

Note that all of the approaches mentioned above require network expansion at each intersection in order to represent all turning movements. However, adding nodes and links to the network to model intersection turning movements is an expensive proposition. Consider a single intersection represented as a node (left figure) as shown in Figure 1, to model the intersection turning movements would require adding 3 nodes and 12 links for each intersection (right figure). For a network with 1,000 nodes and 4,000 links, this would require 4,000 nodes and 16,000 links to fully model all intersection turning movements in the network. This is a fourfold increase in terms of nodes and links. For large-scale networks, this approach is infeasible.

The objective of this study is to propose a methodology to derive complete link flows and turning movement flows for the whole network together with an O–D trip table given traffic counts at selected roads and intersections without the need to expand the network. The idea originated from the concept of path flow estimator (PFE) first proposed by Sherali *et al*. [14] as a linear program based on Wardrop's user equilibrium principle [15]. The PFE is a one-stage network observer that can estimate path flows (hence O–D flows) and path travel times from traffic counts on general road networks. It circumvents the difficulties (*e.g*., non-convexity, convergence issues, etc.) associated with the bi-level programming approach [16,17]. Bell and Shield [18] and Bell *et al*. [19] extended the method to the nonlinear PFE, which is based on the stochastic user equilibrium (SUE) assumptions. The logit-based SUE model allows travelers to choose non-equal travel time paths due to imperfect knowledge of network travel times. In addition, the nonlinear PFE yields unique path flows and does not require all links to be measured. Chen *et al*. [20] applied the nonlinear PFE to examine the quality of synthetic O–D trip table estimated from traffic counts.

The theoretical advantage of the nonlinear PFE is the single-level convex programming formulation with side constraints. Since the objective function is strictly convex with respect to the decision variables (path flows) and the constraints are all linear (equality and inequality) equations, the optimization is guaranteed to yield unique path flows that can be used to derive other useful information at different spatial levels. For example, the sum of all path flows from all O–D pairs gives the total flows utilizing the network, the sum of all path flows emanating from a given origin gives a total trip production, and the sum of path flows terminating at a given destination gives a total trip attraction. Flows between an O–D pair can be obtained by simply adding up the flows on all paths connecting that O–D pair. The aggregated link flows are obtained by adding up all path flows passing through a given link. For the turning movements at an intersection, the orientations of links connected

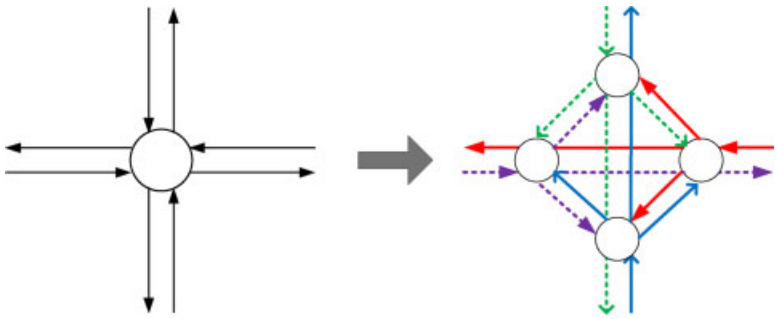

Figure 1. Network representation of an intersection.

DOI: 10.1002/atr

to intersection are needed so as to determine the individual turning movement (*e.g.*, left, right, or through movement) from the used paths without the need to expand the network for representing turning movements. Since the aggregation is a one-to-one mapping, the resulting estimates at different spatial levels (including the turning movement estimates) should be also unique. Note that this uniqueness is different from the under-specified problem of the O–D estimation problem from traffic counts, which is known to have multiple solutions since the number of independent observations (link counts and turning movement counts) is generally less than the number of variables (O–D demands). The multiplicity of the solutions (O–D estimates) should be quantified by some quality measures (*e.g.*, the maximal possible relative error (MPRE), of Yang *et al.* [21], the expected relative error (ERE) of Gan *et al.* [22], or the total demand scale (TDS) of Bierlaire [23].

In this paper, we demonstrate the derivation of turning movements as well as link flows for the whole network *via* PFE with incomplete traffic data for different network topologies. Two case studies utilizing traffic data collected from the City of Logan, Utah, and the City of St. Helena, California, are set up to demonstrate the application of the proposed method. The results also serve to identify the shortcomings and the corresponding improvements for the methodology.

2. PATH FLOW ESTIMATOR WITH TURNING MOVEMENTS

The nonlinear PFE was originally developed by Bell and Shields [18] as a one-stage network observer. It is able to estimate path flows and path travel times using incomplete traffic data from detection devices partially installed in the network. The core component of PFE is a logit-based path choice model in which the perception errors of path travel times are assumed to be independent Gumbel variates [24]. The logit model interacts with link cost functions to produce a SUE traffic pattern. Based on the equivalent formulation for a logit-based SUE problem [25], the PFE formulation with turning movements can be given as follows.

$$\text{Minimize}: \quad Z = \frac{1}{\theta} \sum_{rs \in \text{RS}} \sum_{k \in K_{rs}} f_k^{rs} (\ln f_k^{rs} - 1) + \sum_{a \in A} \int_0^{x_a} t_a(w) \mathrm{d}w \tag{1}$$

subject to:

$$(1-\varepsilon_m^i) \cdot g_m^i \le t_m^i \le (1+\varepsilon_m^i) \cdot g_m^i, \quad \forall\, m \in M_i,\ i \in \bar{I}, \tag{2}$$

$$(1-\varepsilon_a) \cdot v_a \le x_a \le (1+\varepsilon_a) \cdot v_a, \quad \forall\, a \in \bar{A}, \tag{3}$$

$$x_a \le C_a, \quad \forall\, a \in \breve{A}, \tag{4}$$

$$(1-\varepsilon_{rs}) \cdot z_{rs} \le q_{rs} \le (1+\varepsilon_{rs}) \cdot z_{rs}, \quad \forall\, rs \in \overline{\text{RS}}, \tag{5}$$

$$f_k^{rs} \ge 0, \quad \forall k \in K_{rs}, \quad rs \in \text{RS}, \tag{6}$$

where

$$t_m^i = \sum_{rs \in \text{RS}} \sum_{k \in K_{rs}} \sum_{a \in \text{IN}_i} \sum_{b \in \text{OUT}_i} f_k^{rs} \delta_{ak}^{rs} \delta_{bk}^{rs}, \quad \forall\, m \in M_i,\ i \in I, \tag{7}$$

$$x_a = \sum_{rs \in \text{RS}} \sum_{k \in K_{rs}} f_k^{rs} \delta_{ak}^{rs}, \quad \forall\, a \in A, \tag{8}$$

$$q_{rs} = \sum_{k \in K_{rs}} f_k^{rs}, \quad \forall\, rs \in \text{RS}, \tag{9}$$

where $\bar{I}$ and I are the sets of measured and all intersections; M_i is the set of turning movements at intersection i; $\bar{A}$, $\breve{A}$ and A are the sets of measured, unmeasured, and all links ($A = \bar{A} \cup \breve{A}$); $\overline{\text{RS}}$ and RS are the sets of target (or prior) and all O–D pairs; K_{rs} is the set of paths connecting origin r and destination s; θ is the dispersion parameter, IN_i and OUT_i are the sets of links terminating into and originating out of intersection i; ε_m^i, ε_a, and ε_{rs} the measurement errors [0,1] for turning movement m from intersection

DOI: 10.1002/atr

i, flows on link a, and target O–D demands between origin r and destination s; g_m^i and t_m^i are the observed and estimated flows on turning movement m at intersection i; v_a and x_a are the observed and estimated flows on link a; C_a, $t_a(x_a)$ are capacity and cost function of link a; z_{rs} and q_{rs} are the target and estimated O–D flows between origin r and destination s; f_k^{rs} is the estimated flows on path k connecting origin r and destination s; and δ_{ak}^{rs} is the path-link indicator: 1 if link a is on path k between origin r and destination s, and 0 otherwise.

The objective function (1) has two terms: an entropy term and a user equilibrium term. The entropy term seeks to evenly distribute trips to multiple paths according to the dispersion parameter while the user equilibrium term tends to cluster the trips on the minimum cost paths. As opposed to the traditional logit-based SUE model, PFE finds path flows that minimize the SUE objective function in Equation (1) while simultaneously reproducing turning movement counts on all observed intersections in Equation (2), traffic counts on all observed links in Equation (3), and prior travel demands of certain O–D pairs in Equation (5) within some predefined error bounds. For the unobserved links, the estimated flows cannot exceed their capacities as indicated by Equation (4). This constraint is incorporated for the same purpose as in the capacitated traffic assignment [26], which is to prevent producing unrealistically high link flow estimates. Error bounds (ε_m^i, ε_a, and ε_{rs}) are introduced in Equations (2), (3), and (5) to account for measurement errors of turning movement counts, traffic counts, and the confidence associated with prior O–D demands, respectively. More reliable information will constrain the estimation (*e.g.*, turning movement flows, link flows, or O–D flows) to be within a smaller tolerance, whereas less reliable information will allow for a larger deviation. The introduction of the error bounds in Equations (2), (3), and (5) enhances the flexibility of PFE by allowing the user to incorporate local knowledge about the network conditions to the estimation process. Equation (6) constrains the path flows to be non-negativity, while Equations (7), (8), and (9) are definitional constraints to obtain turning movement flows for all intersections, link flows, and O–D flows from the path flow solution.

The Lagrangian function of the PFE formulation and its first partial derivatives with respect to the path-flow variables can be expressed as follows:

$$
\begin{aligned}
L(\mathbf{f},\boldsymbol{\tau},\mathbf{u},\mathbf{d},\mathbf{o}) = Z &+ \sum_{i\in\overline{I}}\sum_{m\in M_i}\tau_m^{i-}\cdot\left(g_m^i(1-\varepsilon_m^i)-\sum_{rs\in\mathrm{RS}}\sum_{k\in K_{rs}}\sum_{a\in\mathrm{IN}(i)}\sum_{b\in\mathrm{OUT}(i)}f_k^{rs}\delta_{ak}^{rs}\delta_{bk}^{rs}\right)\\
&+\sum_{i\in\overline{I}}\sum_{m\in M_i}\tau_m^{i+}\cdot\left(g_m^i(1+\varepsilon_m^i)-\sum_{rs\in\mathrm{RS}}\sum_{k\in K_{rs}}\sum_{a\in\mathrm{IN}(i)}\sum_{b\in\mathrm{OUT}(i)}f_k^{rs}\delta_{ak}^{rs}\delta_{bk}^{rs}\right)\\
&+\sum_{a\in\overline{A}}u_a^-\cdot\left(v_a(1-\varepsilon_a)-\sum_{rs\in\mathrm{RS}}\sum_{k\in K_{rs}}f_k^{rs}\delta_{ak}^{rs}\right)\\
&+\sum_{a\in\overline{A}}u_a^+\cdot\left(v_a(1+\varepsilon_a)-\sum_{rs\in\mathrm{RS}}\sum_{k\in K_{rs}}f_k^{rs}\delta_{ak}^{rs}\right)\\
&+\sum_{a\in\breve{A}}d_a\cdot\left(C_a-\sum_{rs\in\mathrm{RS}}\sum_{k\in K_{rs}}f_k^{rs}\delta_{ak}^{rs}\right)\\
&+\sum_{rs\in\overline{\mathrm{RS}}}o_{rs}^-\cdot\left(z_{rs}(1-\varepsilon_{rs})-\sum_{k\in K_{rs}}f_k^{rs}\right)\\
&+\sum_{rs\in\overline{\mathrm{RS}}}o_{rs}^+\cdot\left(z_{rs}(1+\varepsilon_{rs})-\sum_{k\in K_{rs}}f_k^{rs}\right),
\end{aligned}
\tag{10}
$$

$$
\begin{aligned}
\frac{\partial L}{\partial f_k^{rs}}=0 \;\Rightarrow\; &\frac{1}{\theta}\ln f_k^{rs}+\sum_{a\in A}t_a(x_a)\,\delta_{ak}^{rs}-\sum_{m\in\overline{M}_i}\sum_{i\in\overline{I}}\sum_{a\in\mathrm{IN}_i}\sum_{b\in\mathrm{OUT}_i}\tau_m^{i-}\delta_{ak}^{rs}\delta_{bk}^{rs}-\sum_{m\in\overline{M}_i}\sum_{i\in\overline{I}}\sum_{a\in\mathrm{IN}_i}\sum_{b\in\mathrm{OUT}_i}\tau_m^{i+}\delta_{ak}^{rs}\delta_{bk}^{rs}-\\
&\sum_{a\in\overline{A}}u_a^-\delta_{ak}^{rs}-\sum_{a\in\overline{A}}u_a^+\delta_{ak}^{rs}-\sum_{a\in\breve{A}}d_a\delta_{ak}^{rs}-o_{rs}^--o_{rs}^+=0,\quad\forall\,k\in K_{rs},\ rs\in\mathrm{RS},
\end{aligned}
\tag{11}
$$

DOI: 10.1002/atr

where τ_m^{i-}, τ_m^{i+}, u_a^-, u_a^+, d_a, o_{rs}^-, and $o_{rs}^+$are the dual variables of constraints (2), (3), (4), and (5), respectively. The values of τ_m^{i+}, u_a^+, d_a, and o_{rs}^+ are restricted to be non-positive, while the value of τ_m^{i-}, u_a^- and o_{rs}^-must be non-negative; τ_m^{i-}, τ_m^{i+}, u_a^-, and u_a^+ can be viewed as the corrections to the intersection turning movement delay and link travel time, respectively, by adjusting the estimated path flows to match with the observed turning movement counts and link counts; similarly o_{rs}^- and o_{rs}^+ can be interpreted as corrections to the O–D travel times that can be used to steer the estimated path flow pattern to within the O–D interval constraints specified by Equation (5). These dual variables are zero if the estimated values (*e.g.*, turning movement flows, link flows, and O–D flows) are within an acceptable range defined by the measurement error bound, non-zero if they are binding at one of the limits, and infinity (or very large positive or negative values) if there exists no solution that can fulfill the constraints [19]. Also see Ref. [27] on how to make use of the dual variables to adjust the error bounds if they are initially mis-specified. d_a is related to the link queuing delay when the estimated link flow reaches its capacity [28].

Similar to the logit-based SUE model, path flows can be derived analytically as a function of path cost and dual variables associated with constraints (2), (3), (4), and (5), as follows.

$$f_k^{rs} = \exp\left[\theta\left(\begin{array}{l} -\sum_{a\in A} t_a(x_a)\delta_{ak}^{rs} + \sum_{m\in\overline{M}_i}\sum_{i\in\overline{I}}\sum_{a\in \mathrm{IN}_i}\sum_{b\in \mathrm{OUT}_i}\left(\tau_m^{i-}+\tau_m^{i+}\right)\cdot\delta_{ak}^{rs}\delta_{bk}^{rs}+ \\ \sum_{a\in\overline{A}}\left(u_a^-\delta_{ak}^{rs}+u_a^+\delta_{ak}^{rs}\right) + \sum_{a\in\breve{A}} d_a\delta_{ak}^{rs} + o_{rs}^+ + o_{rs}^- \end{array}\right)\right], \quad \forall\, k\in K_{rs}, \quad rs\in \mathrm{RS} \tag{12}$$

3. SOLUTION ALGORITHM

The solution procedure for solving the PFE with turning movements is depicted in Figure 2. It consists of three main modules: (1) iterative balancing scheme, (2) column (or path) generation, and (3) derivation of turning movements. The basic idea of the iterative balancing scheme is to sequentially scale the path flows to fulfill one constraint at a time by adjusting the dual variables (*e.g.*, τ_m^{i-}, τ_m^{i+}, u_a^-, u_a^+, d_a, o_{rs}^-, and o_{rs}^+). Once the scheme converges, the path flows can be analytically determined by Equation (12). A column generation is included in the solution procedure to avoid path

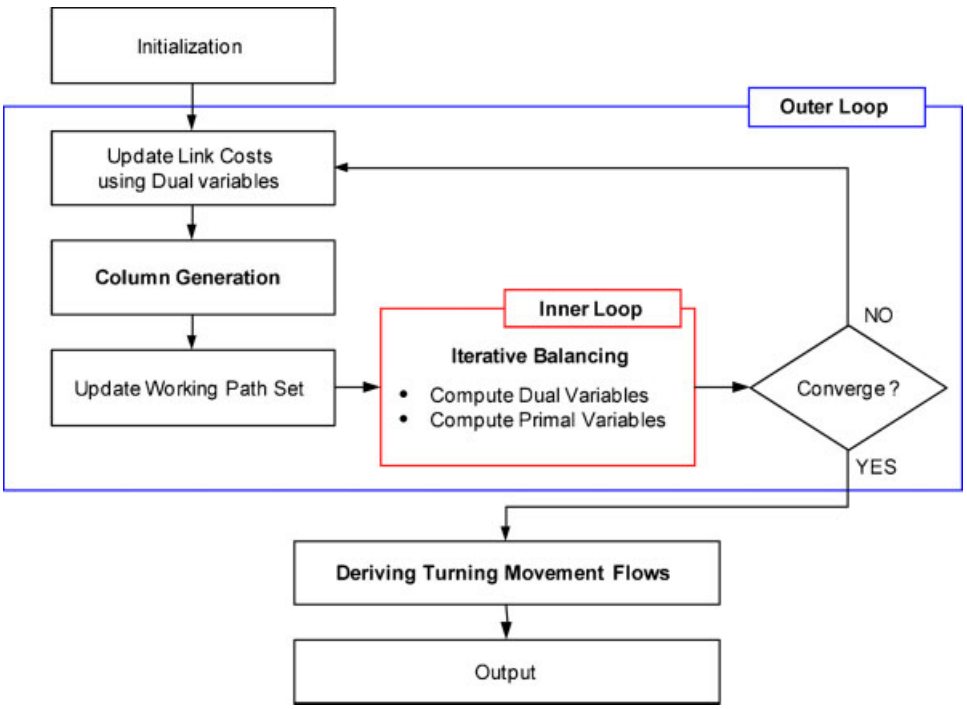

Figure 2. Flowchart of the solution algorithm.

DOI: 10.1002/atr

enumeration for a general transportation network. Finally, an intersection turning movement estimation procedure is used to derive turning movement flows for all intersections (including the unobserved intersections).

3.1. Iterative balancing scheme

The iterative balancing scheme can be summarized as follows.

Step 1. *Initialization*. Set $n=0$, $(\tau_m^{i-})^n$, $(\tau_m^{i+})^n$, $(t_m^{i,n})$, $(u_a^+)^n$, $(u_a^-)^n$, $(d_a)^n$, (x_a^n), $(o_{rs}^-)^n$, $(o_{rs}^+)^n$, and $q_{rs}^n = 0$.

Step 2. *Update Dual Variables and Compute Primal Variables*

a. For each measured intersection ($i \in \bar{\mathrm{I}}$), update the dual variables

$$(\tau_m^{i+})^n = \mathrm{Min}\left\{0, (\tau_m^{i+})^{n-1} + \frac{1}{\theta}\ln\left(\frac{(1+\varepsilon_m^i)\cdot g_m^i}{t_m^i}\right)\right\} \text{ and } (\tau_m^{i-})^n = \mathrm{Max}\left\{0, (\tau_m^{i-})^{n-1} + \frac{1}{\theta}\ln\left(\frac{(1-\varepsilon_m^i)\cdot g_m^i}{t_m^i}\right)\right\}$$

b. For each measured link ($a \in \overline{\mathrm{A}}$), update the dual variables

$$(u_a^+)^n = \mathrm{Min}\left\{0, (u_a^+)^{n-1} + \frac{1}{\theta}\ln\left(\frac{(1+\varepsilon_a)\cdot v_a}{x_a^n}\right)\right\} \text{ and } (u_a^-)^n = \mathrm{Max}\left\{0, (u_a^-)^{n-1} + \frac{1}{\theta}\ln\left(\frac{(1-\varepsilon_a)\cdot v_a}{x_a^n}\right)\right\}.$$

c. For each unmeasured link ($a \in \breve{\mathrm{A}}$), update the dual variables

$$(d_a)^n = \mathrm{Min}\left\{0, (d_a)^{n-1} + \frac{1}{\theta}\ln\left(\frac{C_a}{x_a^n}\right)\right\}.$$

d. For each target O-D flow ($rs \in \overline{\mathrm{RS}}$), update the dual variables

$$(o_{rs}^+)^n = \mathrm{Min}\left\{0, (o_{rs}^+)^{n-1} + \frac{1}{\theta}\ln\left(\frac{(1+\varepsilon_{rs})\cdot z_{rs}}{q_{rs}^n}\right)\right\} \text{ and } (o_{rs}^-)^n = \mathrm{Max}\left\{0, (o_{rs}^-)^{n-1} + \frac{1}{\theta}\ln\left(\frac{(1-\varepsilon_{rs})\cdot z_{rs}}{q_{rs}^n}\right)\right\}$$

Compute path flows using Equation (12), turning movement flows using Equation (7), link flows using Equation (8), and O–D flows using Equation (9).

Step 3. *Convergence Test*.

$$\text{If } \eta_0 \le \mathrm{Max}\left\{\begin{array}{l}\left|(\tau_m^{i+})^n - (\tau_m^{i+})^{n-1}\right|, \left|(\tau_m^{i-})^n - (\tau_m^{i-})^{n-1}\right|, \left|(u_a^+)^n - (u_a^+)^{n-1}\right|, \left|(u_a^-)^n - (u_a^-)^{n-1}\right|, \\ \left|(d_a)^n - (d_a)^{n-1}\right|, \left|(o_{rs}^+)^n - (o_{rs}^+)^{n-1}\right|, \left|(o_{rs}^-)^n - (o_{rs}^-)^{n-1}\right|\end{array}\right\} < \eta,$$

where η_0 is a convergence tolerance (*e.g.*, 10^{-6}) and η is the upper limit of change in dual variables, then set all parameters of the next iteration equal to those of the current iteration, set $n = n+1$, and go to step 2.

$$\text{If } \quad \mathrm{Max}\left\{\begin{array}{l}\left|(\tau_m^{i+})^n - (\tau_m^{i+})^{n-1}\right|, \left|(\tau_m^{i-})^n - (\tau_m^{i-})^{n-1}\right|, \left|(u_a^+)^n - (u_a^+)^{n-1}\right|, \left|(u_a^-)^n - (u_a^-)^{n-1}\right|, \\ \left|(d_a)^n - (d_a)^{n-1}\right|, \left|(o_{rs}^+)^n - (o_{rs}^+)^{n-1}\right|, \left|(o_{rs}^-)^n - (o_{rs}^-)^{n-1}\right|\end{array}\right\} \ge \eta,$$

then set all parameters of the next iteration equal to those of the current iteration, set $n = n+1$, and terminate.

In the above procedure, we just provide the adjustment equations for different types of constraint (*e.g.*, observed intersections, observed links, unobserved links, and target O–D flows). The detailed derivations of the adjustment equations can be found in Refs. [29,30], and convergence of the iterative balancing scheme is discussed in detail in Refs. [19,28].

3.2. Column generation

The above iterative balancing scheme assumes that a working path set is given. For large networks, this is not practical to enumerate a working path set in advance since the number of possible paths grows exponentially with respect to network size. To circumvent path enumeration, a column (or path) generation procedure can be augmented to the iterative balancing scheme. Basically, the algorithm introduces an outer loop (or iteration) to iteratively generate paths to the working path set as needed to replicate the observed link counts, turning movement counts, and selected prior O–D flows, and to

DOI: 10.1002/atr

account for the capacity restraints for the unobserved links and congestion effects, while the iterative balancing scheme iteratively adjusts the primal variables (path flows, link flows, intersection turning movement flows, and O–D flows) and the dual variables in the inner loop for a given working path set from the outer loop. Note that the working path set is generated by a column generation scheme (or a shortest path algorithm) using the generalized link costs, which is based on not only the link costs but also the dual variables from the active side constraints in Equations (2)–(5). The dual variables force the column generation scheme to generate paths that satisfy the side constraints. See Refs. [19,29,30] for additional discussions on the issue of using the generalized link costs to generate paths.

3.3. Derivation of turning movements

In order to derive intersection turning movements from path flows, links emanating from and terminating to the intersection should be grouped into a set of inbound and outbound links as shown in Figure 3. These sets will be used in Equation (7) to derive intersection turning movement flows from path flows as follows.

Step 0. Set $t_m^i = 0, \quad \forall i, m$
Step 1. Set $rs = 1$.
Step 2. Set $k = 1$.
Step 3. For path k, if the ending node of link a is intersection i, then set IN $= a$, OUT= next link b after link a in path k, and $t_m^i = t_m^i + f_k^{rs}$.
Step 4. If $k < |K_{rs}|$, set $k = k + 1$ and go to step 3, otherwise go to step 5.
Step 5. If $rs < |\mathrm{RS}|$, set $rs = rs + 1$ and go to step 2, otherwise go to step 6.
Step 6. If $m < |M_i|$, set $m = m + 1$ and go to step 1, otherwise terminate.

By incorporating the above procedure into PFE, flows on each intersection turning movement can be obtained as part of the estimation results (together with path flows, link flows, and O–D flows).

4. NUMERICAL RESULTS

To demonstrate the PFE model with turning movements and solution algorithm for deriving intersection turning movements, two networks are adopted in the numerical experiments. First, a signalized arterial network is used to illustrate the application of a linear network for estimating turning movement flows. Then, the St. Helena network is employed to demonstrate the incorporation of intersection turning movements for selected intersections as observed interval constraints to improve

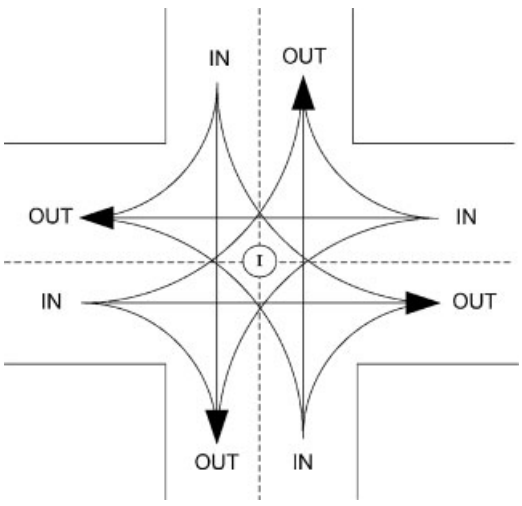

Figure 3. Link grouping example.

DOI: 10.1002/atr

the estimation. Accuracy of the estimates can be measured by the root mean square error (RMSE) as follows:

$$\mathrm{RMSE} = \sqrt{\frac{1}{N}\sum_{n=1}^{N}(x_{\mathrm{est}}^{n} - x_{\mathrm{obs}}^{n})^{2}} \tag{13}$$

where N is the number of observations, x_{est} and x_{obs} are the estimated and observed link (or turning movement) flows, respectively.

4.1. A signalized arterial

The first example considers an arterial street connected by a series of signalized intersections. The layout of this arterial as well as the traffic counts are provided in Figure 4. Traffic counts were collected during the evening peak hour. Data preprocessing were required to remove errors and inconsistencies in order to avoid getting erroneous results. This network involves 8 signalized intersections, 50 links, 18 external stations, and 306 O–D pairs. The total demand of this network is 12,110 vehicles. The dispersion parameter of this network is assumed to be 8 hour^{-1}. This parameter measures the degree of dispersion in the network, which is related to the perception variance of the travelers (*i.e.*, familiarity with the network). It is network specific, and should be calibrated based on real-world data (see Refs. [19,31] for details on the data requirements and the calibration procedure). The delay of each movement is assumed to be different but constant according to Table I. The delays for prohibited movements (*e.g.*, direction 1 and then direction 3) are set to a very large number in order to prevent such illegal movements. In this example, we assume that the travel delay pattern at all intersections is identical. These movement delays are included in the path travel time calculations used to update the path flows in Equation (12). These turning penalties serve as an additional cost used to penalize paths with many turns (*i.e.*, similar to the commonality factor used in the C-logit model [32,33] to penalize paths that are not fully independent). Traffic counts on links originating from and terminating to the external stations, 36 out of 50 links, are used as observation constraints. The O–D demand estimates are presented in Table II.

As can be seen from Table II, the total demand of this network can be estimated correctly since all entry and exit flows are provided. The observations on entry and exit links represent trip productions at origins and trip attractions at destinations in the sense of a trip distribution procedure. These numbers are matched exactly since they are used as observation constraints in the PFE model. Because of the unavailability of

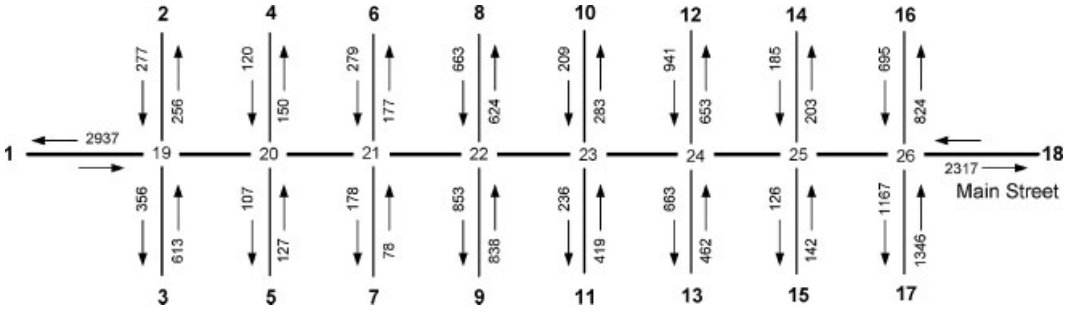

Figure 4. Layout of arterial network with entry and exit flow observations.

Table I. Intersection turning movement delays (turn penalties).

Approach	Delay (hour) 1 (NB)	2 (EB)	3 (SB)	4 (WB)
1 (NB)	0.017	0.017	∞	0.024
2 (EB)	0.030	0.020	0.020	∞
3 (SB)	∞	0.024	0.017	0.017
4 (WB)	0.020	∞	0.030	0.020

DOI: 10.1002/atr

Table II. O–D trip table estimated using observations on entry and exit links.

From/To	1	2	3	4	5	6	7	8	9	10	11	12	13	14	15	16	17	18	Total
1		178	243	87	59	83	76	238	308	79	62	152	133	33	18	104	148	426	2428
2	196		8	3	2	3	3	9	11	3	2	5	5	1	1	4	5	15	277
3	451	12		6	4	6	6	18	23	6	5	11	10	2	1	8	11	32	613
4	71	2	3		1	2	2	5	7	2	1	3	3	1	0	2	3	10	120
5	78	2	4	2		2	2	5	7	2	1	3	3	1	0	2	3	9	127
6	133	4	6	3	3		5	17	23	6	5	11	10	2	1	8	11	31	279
7	39	1	2	1	1	1		5	6	2	1	3	3	1	0	2	3	8	78
8	260	7	12	6	5	10	11		71	19	15	37	32	8	4	25	36	103	663
9	357	10	16	9	7	14	15	65		24	19	45	40	10	5	31	44	127	838
10	61	2	3	1	1	2	3	12	18		6	15	13	3	2	10	15	42	209
11	129	4	6	3	2	5	6	25	38	13		28	25	6	3	19	27	79	419
12	221	6	10	5	4	9	10	43	65	24	23		77	20	11	63	90	259	941
13	114	3	5	3	2	5	5	22	34	13	12	39		9	5	29	42	120	462
14	31	1	1	1	1	1	1	6	9	3	3	11	12		3	15	22	63	185
15	25	1	1	1	0	1	1	5	7	3	3	9	9	3		11	16	45	142
16	93	3	4	2	2	4	4	18	27	10	10	34	35	13	8		106	322	695
17	202	6	9	5	4	8	9	39	59	22	21	74	76	27	18	141		626	1346
18	473	14	22	11	9	19	20	92	139	52	48	172	178	64	42	349	584		2288
Total	2937	256	356	150	107	177	178	624	853	283	236	653	663	203	126	824	1167	2317	12 110

the true O–D trip table, we do not report the RMSE for the O–D estimates; instead we report the RMSE for the estimated turning movements. The estimated turning movements are depicted in Figure 5.

For this case study, it is found that the turning movement estimates on the major street are acceptable while those on the minor streets are not, especially for the through movements. In general, the through movement estimates on the minor streets are underestimated while their left- and right-turn counterparts are overestimated. This is due to the fact that there is only one path traversing the through movements on any minor streets (*e.g.*, path from node 3 to node 2 in Figure 4) while there is at least one path traversing the other movements (from minor street to major street). In addition, since the main traffic stream is on the major street, the contribution of flows from one minor street (through movement) to match the observation on the opposite minor street is always dominated by the flows from the major street

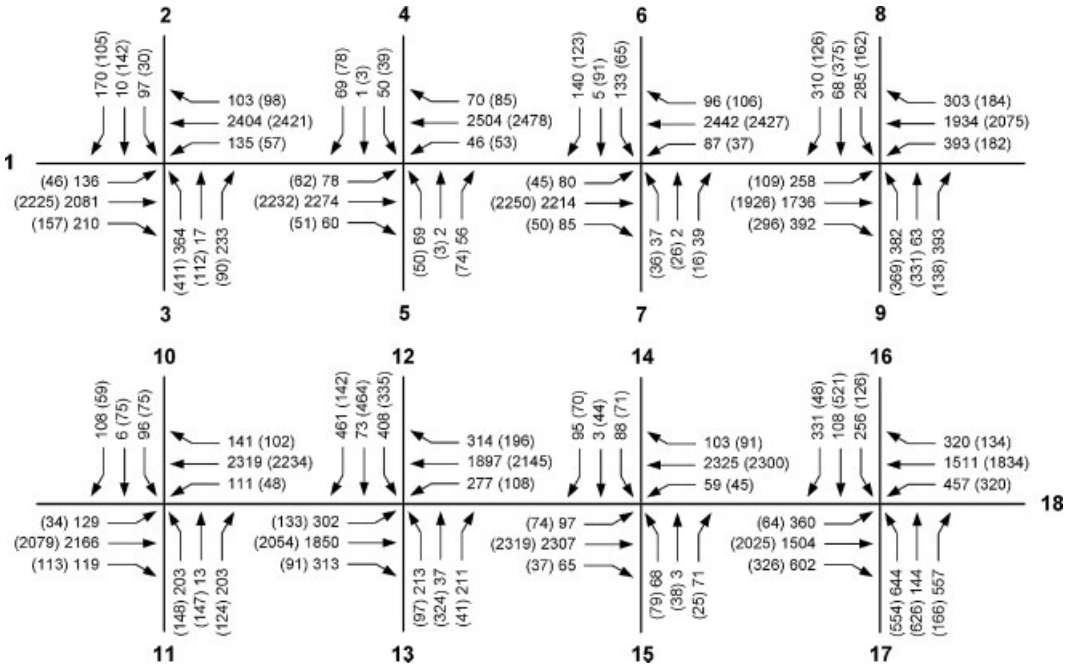

Figure 5. Estimated (Observed) turning movements for arterial network ($RMSE_{turn} = 209.048$).

DOI: 10.1002/atr

especially when the turn penalties at intersection are likely to be mis-specified. The observed (in parenthesis) and estimated turning movement flows are shown in Figure 5 for comparison.

4.2. St. Helena network

The City of St. Helena is located in the famous wine-producing region of Napa Valley in California, approximately 65 miles north of San Francisco. St. Helena is a full service City with a population of 6,019 (as of January 1, 2002) within an area of 4 square miles. The City's development pattern is relatively compact, with commercial development and wineries concentrated along Highway 29 (Main Street) corridor, and residential development radiating out from Main Street (see Figure 6).

Link volumes collected during the evening peak hour, the time of day when traffic congestion on Highway 29 presents a serious issue, were assembled and a network with 28 TAZs was coded with the observed link volumes. The network contains 113 links and 54 of the links do not have traffic count data. Turn penalties, based on the actual traffic conditions, were also coded with the network such that the shortest paths among TAZ centroids replicate actual travel patterns in the area. PFE was applied to the network for estimation of the O–D table as well as turning movements.

For this set of experiments, link counts were aggregated from turning movement counts. As a result, there are link counts on all approaches (both in-bounds and out-bounds) of each intersection. In addition, turning movement counts at two intersections (Fulton/Main and Mitchell Dr./Oak Avenue) were also considered to assist the estimation (used as constraints in addition to link observation constraints). The following three sets of traffic counts were used for the estimations.

1. Link counts only (Base case).
2. Base case plus turning counts at Fulton/Main (Option A).
3. Option A plus turning counts at Mitchell Dr./Oak Avenue (Option B).

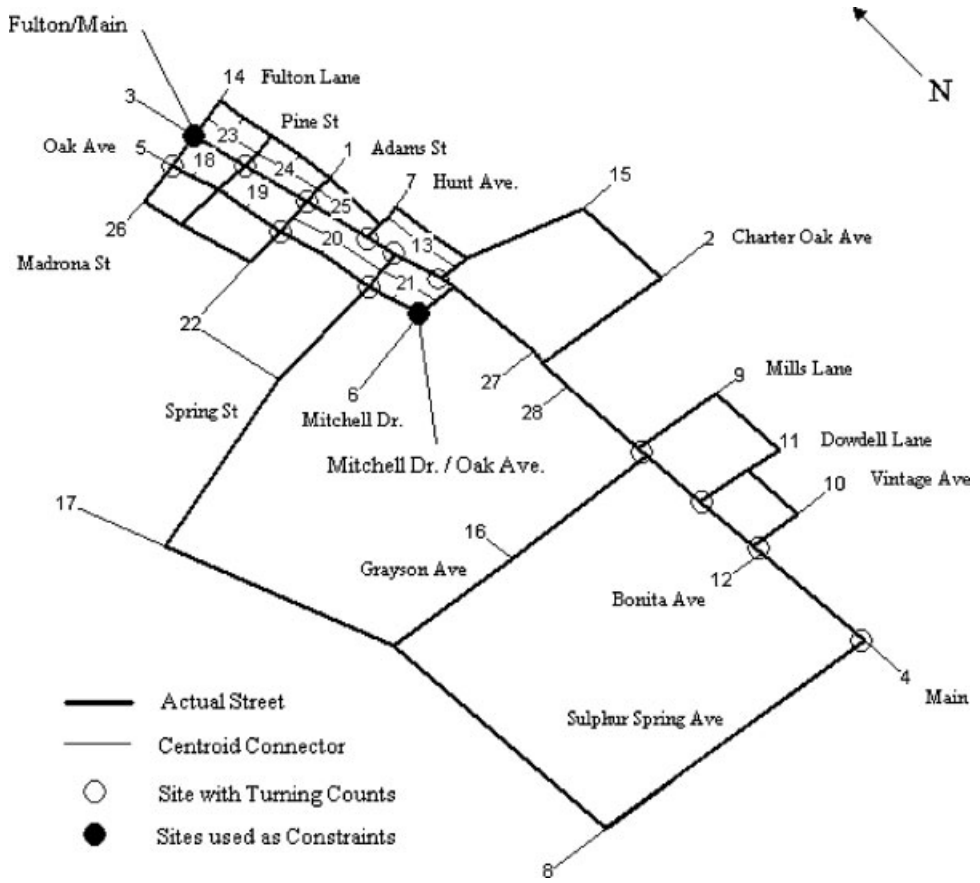

Figure 6. Topology of St. Helena network and locations of intersection turning movement counts.

DOI: 10.1002/atr

Table III. Numbering systems, names, and observed intersection turning movement counts.

ID	Name	Observation											
		NBL	NBT	NBR	SBL	SBT	SBR	EBL	EBT	EBR	WBL	WBT	WBR
31	Fulton Ln and Main	46	609	32	32	563	70	148	46	13	8	27	158
32	Sulphur Spring Ave and Main	81	817			844	35	7		72			
33	Madrona St and Oak Avenue	36	25	93	9	22	2	4	145	75	83	81	7
34	Mitchell Dr and Oak Avenue				241		11	35	33			31	140
40	Bonita Ave and Main	30	794			858	49	19		21			
68	Mills Ln and Main		841	3	5	841					6		4
70	Grayson Ave and Main	125	807			760	87	37		78			
71	Dowdell Ln and Main		735	45	48	790					42		167
73	Pine St and Main	1	685	13	4	570	10	1		16	3	1	1
75	Adams St and Main	43	607	40	67	490	32	60	118	27	72	58	32
77	Adams St and Oak Avenue	18	139	111	26	167	10	12	47	26	76	41	35
78	Hunt Ave and Main		504	141	41	637					24		36
80	Spring St and Oak Avenue	39	160	12	36	213	44	62	52	59	13	63	49
81	Spring St and Main	93	623			598	63	22		72			
82	Mitchell Dr and Main		607	63	93	602					232		109
86	Vintage Ave and Main		742	71	30	823					84		66

For these sets of data, there exists flow inconsistency; the total inflow is not equal to the total outflow at some intersections, especially at Fulton/Main and Madrona Street/Oak Avenue. The westbound outflow from Fulton/Main (143 units) is quite different from the observed westbound inflow at Madrona Street/Oak Avenue (171 units), about 17 percent error. For adjusting the measurement errors of link counts, it was assumed that the turning movement counts at Fulton/Main and Mitchell Dr./Oak Avenue intersections are error-free. The measurement errors of individual link counts were adjusted differently dependent on their difficulty in matching the counts. These errors vary from 0 to 17 percent of actual link counts.

Figure 6 depicts the map of St. Helena network and locations of two intersections (black circles) of which turning movement counts were considered to assist the estimation. The turning movement counts at other intersections (hollow circles) were also collected for comparison purposes. Table III summarizes the numbering systems, names, and observed turning movement counts of all considered intersections.

Table IV summarizes the estimation results in terms of link flow and turning flow estimates. Since the same error bounds were used for all link measurements in all three cases, there is no significant difference in terms of replicating the observed link counts. The maximum error of estimated link flows is about 17 percent, while the RMSEs are about the same for all cases. However, it can be observed that the ability of matching link counts is slightly deteriorated (higher RMSE) when turning movement counts were also considered in the estimation. From Figure 7, it is found that, for all three cases, about 46–47 percent of estimated link flows are within ± 3 percent of observed values, and almost all estimated link flows (98–99 percent) are within ± 12 percent of the observed values.

From Table IV (second column), when the turning movement counts were incorporated into the estimation, the accuracies of turning flow estimates are generally improved. The RMSE is reduced from 39.61 in the base case to 33.59 in Option A, and to 28.89 in Option B. The results imply the benefit of incorporating partial turning movement counts in the estimation. However, the maximum errors of estimated turning movement flows could be very large ($\approx$1,000 percent), this is due to the fact that many small-observed turning movement volumes (*e.g.*, 1 unit of flow) are highly overestimated. About

Table IV. Accuracies of link flow and turning movement estimates.

Option	Link flows		Turning movements	
	RMSE	Max error (percent)	RMSE	Max error (percent)
Base Case	27.13	17	39.61	901
Option A	27.15	17	33.59	1053
Option B	27.27	17	28.89	1234

DOI: 10.1002/atr

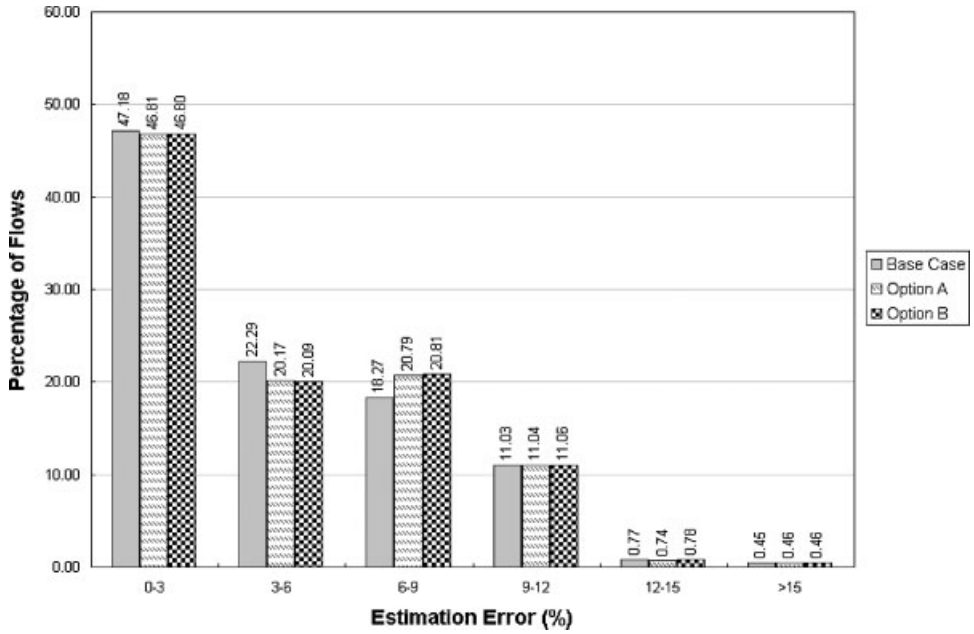

Figure 7. Estimation errors of link flow estimates.

73 percent of turning movement flows estimated in the base case, 80 percent of turning movement flows estimated in Option A, and 76 percent of turning movement flows estimated in Option B are within ± 12 percent of the observed values.

Figures 8a, 8b, and 8c display the estimation errors of turning movement flows at different flow levels for the base case, Option A, and Option B, respectively. For all three cases, majority of the

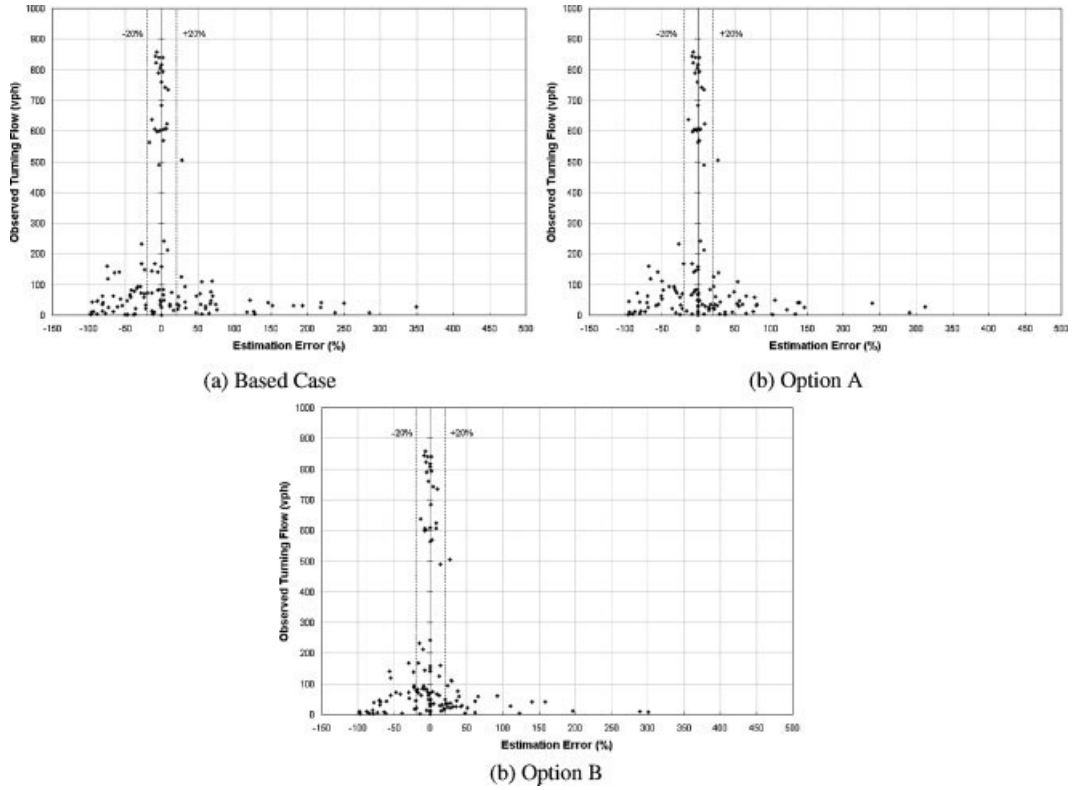

Figure 8. Estimation errors of the intersection turning movement flows estimated for all three cases.

DOI: 10.1002/atr

high-observed turning movement volumes (*e.g.*, ≥ 200 vph; more important) can be estimated within ± 20 percent of the observed values. These figures also reveal the fact that a lot of the small-observed turning movement volumes are highly overestimated (*e.g.*, >100 percent).

5. CONCLUDING REMARKS

In this paper, we demonstrated how to derive complete link and turning movement estimates for the whole network together with O–D trip table given some link counts and intersection turning movement counts *via* the nonlinear PFE. In particular, we suggested an approach to derive intersection turning movement flows without the need to expand the network. Two case studies with actual traffic count data were used to test the intersection turning movement estimation using PFE. The results obtained from the case studies are encouraging. PFE can estimate link volumes and turning movement flows within an acceptable error bound. It is also found that estimation accuracy is better when more link traffic counts (and intersection turning movement counts) are available. Despite the promising results, additional work is needed to investigate the PFE model with more case studies and to refine the PFE to better model the turning movements, leading to the improvement of the quality of O–D estimates as a whole.

6. LIST OF SYMBOLS AND ABBREVIATIONS

6.1. Symbols

$\overline{\mathrm{I}}$, I	Sets of measured and all intersections
M_i	Set of turning movements at intersection i
$\overline{\mathrm{A}}$, $\breve{\mathrm{A}}$, A	Sets of measured, unmeasured, and all links ($\mathrm{A}=\overline{\mathrm{A}}\cup\breve{\mathrm{A}}$)
$\overline{\mathrm{RS}}$, RS	Sets of target (or prior) and all O-D pairs
K_{rs}	Set of paths connecting origin r and destination s
θ	Dispersion parameter
IN_i, OUT_i	Sets of links terminating into and originating out of intersection i
ε_m^i, ε_a, ε_{rs}	Measurement errors [0,1] for turning movement m from intersection i, flows on link a, and target O-D demands between origin r and destination s
g_m^i, t_m^i	Observed and estimated flows on turning movement m at intersection i
v_a, x_a	Observed and estimated flows on link a
C_a, $t_a()$	Capacity and cost function of link a
z_{rs}, q_{rs}	Target and estimated O-D flows between origin r and destination s
f_k^{rs}	Estimated flows on path k connecting origin r and destination s
δ_{ak}^{rs}	Path-link indicator: 1 if link a is on path k between origin r and destination s, and 0 otherwise
x_{est}, x_{obs}	Estimated and observed link or turning movement flows

6.2. Abbreviations

PFE	Path Flow Estimator
NETFLO	Network Flow
O-D	Origin-Destination
SUE	Stochastic User Equilibrium
MPRE	Maximal Possible Relative Error
ERE	Expected Relative Error
TDS	Total Demand Scale
RMSE	Root Mean Square Error

ACKNOWLEDGEMENTS

This research was supported in part by the California Partners for Advanced Transit and Highways (PATH) Program through a grant (TO 5502). The contents of this paper reflect the views of the authors

DOI: 10.1002/atr

who are responsible for the facts and the accuracy of the data presented herein and do not necessarily reflect the views of our sponsor. Constructive comments and suggestions provided by two anonymous referees are highly appreciated.

REFERENCES

1. Caltrans. ''Guide for the preparation of traffic impact studies'', Caltrans, State of California, Department of Transportation. December 2002. http://www.dot.ca.gov/hq/traffops/developserv/operationalsystems/reports/tisguide.pdf
2. Furness KP. Time function iteration. *Traffic Engineering and Control* 1965; **7**(7): 458–460.
3. Jeffreys M, Norman M. On finding realistic turning flows at road junctions. *Traffic Engineering and Control* 1977; **18**(1): 19–25.
4. Mekky A. On estimating turning flows at road junctions. *Traffic Engineering and Control* 1979; **20**(10): 486–487.
5. van Zuylen HJ. The estimation of turning flows on a junction. *Traffic Engineering and Control* 1979; **20**(11): 539–541.
6. Hauer E, Pagitsas E, Shin BT. Estimation of turning flows from automatic counts. *In Transportation Research Record* 1981; **795**: 1–7.
7. Bell MGH. The estimation of junction tuning movements from traffic counts: the role of prior information. *Traffic Engineering and Control* 1984; **25**(5): 279–283.
8. Maher MJ. Estimating the turning flows at a junction: A comparison of three models. *Traffic Engineering and Control* 1984; **25**(1): 19–22.
9. Schaefer MC. Estimation of intersection turning movements from approach counts. *ITE Journal* 1988; **58**(10): 41–46.
10. Martin PT, Bell MC. Network programming to derive turning movements from link flows. *Transportation Research Record* 1992; **1365**: 147–154.
11. Martin PT. Turning movement estimation in real time. *Journal of Transportation Engineering* 1997; **123**(4): 252–260.
12. Wu JH, Thnay C. An O–D based method for estimating link and turning volume based on counts. *Paper presented at ITE District 6 Annual Meeting*, July 8–11, New Mexico, 2001.
13. Spiess H. ''A Gradient Approach for the O–D Matrix Adjustment Problem'' *CRT-693*, 1990. http://www.inro.ca/en/pres_pap/international/ieug90/Paper01_ 1990.pdf
14. Sherali HD, Sivanandan R, Hobeika AG. A linear programming approach for synthesizing origin–destination trip tables from link traffic volumes. *Transportation Research Part B* 1994; **28**(3): 213–234.
15. Wardrop JG. Some theoretical aspects of road traffic research. *Proceedings of the Institution of Civil Engineering*, Part II (1), U.K. 1952: pp. 325–378.
16. Yang H, Iida Y, Sasaki T. Estimation of origin–destination matrices from traffic counts on congested networks. *Transportation Research Part B* 1992; **26**(6): 417–434.
17. Maher M, Zhang X, van Vliet D. A bi-level programming approach for trip matrix estimation and traffic control problems with stochastic user equilibrium link flows. *Transportation Research Part B* 2001; **35**(1): 23–40.
18. Bell MGH, Shield CM. A log-linear model for path flow estimation. *Proceedings of the 4th International Conference on the Applications of Advanced Technologies in Transportation Engineering*, Carpi, Italy, 1995: pp. 695–699.
19. Bell MGH, Shield CM, Busch F, Kruse G. A stochastic user equilibrium path flow estimator. *Transportation Research Part C* 1997; **5**(3/4): 197–210.
20. Chen A, Chootinan P, Recker W. Examining the quality of synthetic origin–destination trip table estimated by path flow estimator. *Journal of Transportation Engineering* 2005; **131**(7): 506–513.
21. Yang H, Iida Y, Sasaki T. An analysis of the reliability of an origin–destination trip matrix estimated from traffic counts. *Transportation Research Part B* 1991; **25**(5): 351–363.
22. Gan L, Yang H, Wong SC. Traffic counting location and error bound in origin–destination matrix estimation problems. *Journal of Transportation Engineering* 2005; **131**(7): 524–534.
23. Bierlaire M. The total demand scale: a new measure of quality for static and dynamic origin–destination trip tables. *Transportation Research Part B* 2002; **36**(9): 755–851.
24. Dial R. A probabilistic multipath traffic assignment model that obviates path enumeration. *Transportation Research* 1971; **5**: 83–113.
25. Fisk C. Some developments in equilibrium traffic assignment. *Transportation Research Part B* 1980; **14**(3): 243–255.
26. Larsson T, Patriksson M. An augmented Lagrangian dual algorithm link capacity side constrained traffic assignment problems. *Transportation Research Part B* 1995; **29**(6): 433–455.
27. Chootinan P, Chen A, Recker W. Improved path flow estimator for estimating origin–destination trip tables. *Transportation Research Record* 2005; **1923**: 9–17.
28. Bell MGH, Iida Y. *Transportation Network Analysis*. Wiley: New York, 1997.

DOI: 10.1002/atr

29. Chen A, Chootinan P, Recker W. Norm approximation method for handling traffic count inconsistencies in path flow estimator. *Transportation Research Part B* 2009; **43**(8): 852–872.
30. Chen A, Ryu S, Chootinan P. L_∞-norm path flow estimator for handling traffic count inconsistencies: Formulation and solution algorithm. *ASCE Journal of Transportation Engineering* 2010; **136**(6): 565–575.
31. Sheffi Y. *Urban Transportation Networks: Equilibrium Analysis with Mathematical Programming Methods*. Prentice-Hall, Incorporated, Englewood Cliffs: NJ, 1985.
32. Cascetta E, Nuzzolo A, Russo F, Vitetta A. A modified logit route choice model overcoming path overlapping problems: specification and some calibration results for interurban networks. *Proceedings of the International Symposium on Transportation and Traffic Theory*, Lesort JB, editor, Lyon (France), 1996: pp. 697–711.
33. Zhou Z, Chen A, Behkor S. C-logit stochastic user equilibrium model: formulations and solution algorithm. *Transportmetrica* (in press).

DOI: 10.1002/atr